Rapport de Stage de Master 2
Spécialité: Physique Subatomique et Astroparticules

New resonances at the LHC

présenté par

Tomáš Ježo

N° Etudiant: 20807557
Email: tomas@he.sk

15 juin 2009

Maîtres de stage	Dr. I. Schienbein
	Prof. M. Klasen
Rapporteur	Dr. S. Kraml

Abstract

In this document we describe a novel implementation for the simulation of a general W$'$-boson in the leading order Monte Carlo generator `PYTHIA` [1]. The Lagrangian for a general charged vector boson is introduced and the model-independent differential cross section computed. A brief review of the Standard Model extensions based on an enlarged group predicting the W$'$ together with their constraints from the electro-weak precision data is offered. Furthermore, we include the description of our extension of `PYTHIA` which generalizes the W$'$-boson to account for the diversity of the existing models and in particular accounts for the interference of the W$'$-boson with the Standard Model W-boson. We demonstrate the use of the improved MC generator and show the numerical results for transverse mass distributions and charge asymmetries within different models containing a W$'$-boson.

Contents

Chapter 1

Introduction

There is no experimental data that unequivocally runs counter to the predictions of the Standard model of particle interactions (SM) based on the $SU(3)_C \times SU(2)_L \times U(1)_Y$ gauge group. It is reasonable, however, to ask if a model based on an enlarged gauge group can be constructed. The fact that in the SM left-handed (right-handed) quarks and leptons transform as doublets (singlets) under the same $SU(2)_L \times U(1)_Y$ gauge group has four important implications: (1) the right-handed particles have no weak interactions, (2) the observed weak-interaction strength of quarks is equal to that of leptons, (3) the observed weak-interaction strength of each generation of quarks and leptons is equal to one another and (4) the charged-current strength is equal to the neutral-current strength (as long as $SU(2)_L \times U(1)_Y$ is spontaneously broken only by scalar doublets). When new data from the Large Hadron Collider (LHC) will be available, it might become obvious that the SM represents only a low-energy limit of more complicated scenario. It is therefore theoretically desirable to have a natural framework for describing any possible deviations of the SM predictions with experimental data.

Since many extensions of the SM predict a spin-1 neutral resonance mediating neutral currents, generically denoted as Z', a huge theoretical and experimental effort was invested in studies of new signals of Z' at LHC. On the other hand W'-bosons, generically identified as charged spin-1 resonances, were given much less attention. And since wherever a W'-boson is predicted there is also a Z'-boson studies involving W'-bosons are desired. Furthermore, research on W'-boson and Z'-boson correlations is very well motivated.

This report presents a guide on how to get started with studying a general W'-boson in a leading order general purpose Monte Carlo generator PYTHIA [1]. For that purpose we offer its extension containing W' which interferes and mixes with Standard Model's W (W^{SM}). On the top of that we give user the possibility to set generation and quark-lepton nonuniversal couplings of the implemented W' as well as the right-handed mixing matrix. This extension has its limitations though, as we focus mainly on the $l + \not{E}_T$ channel, i.e. processes with leptonic final states have been implemented.

The document is organized as follows. In the second chapter a general model-independent W' is introduced. This is followed by a review of the theories with an additional charged vector boson. The third chapter is devoted to leading order computation of the differential cross section of charged vector boson production at hadron colliders. In Chapter 4 we offer a short description of how PYTHIA was extended together with a user manual of new features. Chapter 5 contains the discovery limits and a few signal characteristics for W'-boson predicted by models discussed in Chapter 2. And finally, the last chapter contains the conclusions together an outlook of possible follow-up work.

Chapter 2

Theories with an additional charged vector boson

Beside the theories predicting an additional charged bosons with a W'-like behaviour such as Kaluza-Klein excitations in models with extra dimensions, Technicolor or Supersymmetry, the most common theories of new physics with an additional W'-boson are the extensions of the SM with an enlarged gauge group. Because of the limited time for this research project, we will focus our attention only on the latter. The former, however, present very interesting possibilities and we plan to investigate their predictions for charged boson production and decay at LHC in a follow-up of this work.

2.1   Couplings to the SM fermions

The interaction of a general W' boson with Standard Model (SM) fermions can be written as [2]:

$$\mathcal{L}_{cc}^{\mathrm{W}'} = \frac{g_W}{\sqrt{2}} \left[\overline{\mathrm{u}}_i \gamma^\mu \left((U_{\mathrm{CKM}}^L)_{ij} C_{q_{jk}}^L P_L + (U_{\mathrm{CKM}}^R)_{ij} C_{q_{jk}}^R P_R \right) \mathrm{d}_k + \overline{\nu}_j \gamma^\mu \left(C_{l_{jk}}^L P_L + C_{l_{jk}}^R P_R \right) \mathrm{e}_k \right] \mathrm{W}'_\mu + \mathrm{h.c.}.$$

(2.1)

Here, $\frac{g_W}{\sqrt{2}} = \frac{e}{\sqrt{2}\sin\theta_W} = \frac{1}{2} \left(\frac{G_F M_W^2}{\sqrt{2}} \right)^{\frac{1}{2}}$ is the weak gauge coupling, u, d, ν, and e are the SM fermions in the mass eigenstate basis, $i, j, k = 1, 2, 3$ label the fermion generation, U_{CKM}^L is the Cabibbo–Kobayashi–Maskawa (CKM) matrix, U_{CKM}^R its right-handed equivalent[1] and $P_{L,R} = (1 \mp \gamma^5)/2$ are the projectors onto left- and right-handed chiral fields. The C_q^L, C_q^R, C_l^L, and C_l^R are in general dimensionless diagonal matrices with complex entries. If the right-handed leptonig coupling is non-zero $C_{l_{ii}}^R \neq 0$, then the ith generation includes a right-handed neutrino $\nu_{iR} = P_R \nu_i$.

In the equation above, it is common to separate the chiral operator γ^5 term. As this convention is employed in the PYTHIA manual [1], let us take a look on what the former formula reads in this convention. Using the definition of the projectors $P_{L,R}$ the interactions of a W' can be rewritten

---

[1]The lepton mixing doesn't play a role here, since neutrinos cannot be in the current collider experiments detected.

3

as:

$$\mathcal{L}_{cc}^{\mathrm{W}'} = \frac{1}{2}\frac{g_W}{\sqrt{2}}\left[\overline{\mathrm{u}}_i\gamma^\mu\left\{\left[(U_{\mathrm{CKM}}^L)_{ij}C_{q_{jk}}^L + (U_{\mathrm{CKM}}^R)_{ij}C_{q_{jk}}^R\right] - \left[(U_{\mathrm{CKM}}^L)_{ij}C_{q_{jk}}^L - (U_{\mathrm{CKM}}^R)_{ij}C_{q_{jk}}^R\right]\gamma^5\right\}\mathrm{d}_k \right.$$

$$\left. + \overline{\nu}_i\gamma^\mu\left\{\left[C_{l_{jk}}^L + C_{l_{jk}}^R\right] - \left[C_{l_{jk}}^L - C_{l_{jk}}^R\right]\gamma^5\right\}\mathrm{e}_j\right]\mathrm{W}'_\mu + \mathrm{h.c.} .$$

(2.2)

PYTHIA offers two different particles with W'-like behaviour. One of these particles is $\mathrm{W_L}$, in PYTHIA denoted originally as W', and its flavour code (KF) is 34. Even though it is possible to set up its right-handed couplings so that they are non-zero, $C_{q(l)}^R \neq 0$, it is not implemented to couple to the right-handed neutrinos at all. In our case, therefore, it represents the left-handed component of a W'. The other particle, in PYTHIA denoted as $\mathrm{W_R}$ (KF=9900024), is purely right-handed in the view that it does not couple to the left-handed neutrinos. Hence it can be used as the right-handed component of a general W'. The previous equation can be easily expressed in terms of the left- and right-component, $\mathrm{W_L}$ and $\mathrm{W_R}$, in the following way:

$$\mathcal{L}_{cc}^{\mathrm{W}'} = \frac{g_W}{2\sqrt{2}}\left[\overline{\mathrm{u}}_i(U_{\mathrm{CKM}}^L)_{ij}\gamma^\mu\left(C_{q_{jk}}^{V,\mathrm{W_L}} - C_{q_{jk}}^{A,\mathrm{W_L}}\gamma^5\right)\mathrm{d}_k + \overline{\nu}_i\gamma^\mu\left(C_{l_{jk}}^{V,\mathrm{W_L}} - C_{l_{jk}}^{A,\mathrm{W_L}}\gamma^5\right)\mathrm{e}_j\right]\mathrm{W_{L\mu}}$$

$$+ \frac{g_W}{2\sqrt{2}}\left[\overline{\mathrm{u}}_i(U_{\mathrm{CKM}}^R)_{ij}\gamma^\mu\left(C_{q_{jk}}^{V,\mathrm{W_R}} - C_{q_{jk}}^{A,\mathrm{W_R}}\gamma^5\right)\mathrm{d}_k + \overline{\nu}_i\gamma^\mu\left(C_{l_{jk}}^{V,\mathrm{W_R}} - C_{l_{jk}}^{A,\mathrm{W_R}}\gamma^5\right)\mathrm{e}_j\right]\mathrm{W_{R\mu}} \quad (2.3)$$

$$+ \mathrm{h.c.} ,$$

where the matrices $C_{q(l)}^{V,A}$ are defined as

$$C_{q(l)_{jk}}^{V,\mathrm{W_L}} = C_{q(l)_{jk}}^{A,\mathrm{W_L}} = C_{q(l)_{jk}}^L , \qquad\qquad C_{q(l)_{jk}}^{V,\mathrm{W_R}} = -C_{q(l)_{jk}}^{A,\mathrm{W_R}} = C_{q(l)_{jk}}^R . \qquad (2.4)$$

The definitions above will come in handy when rewriting couplings of various W' predicted in different models, where they are usually not given in the V-A notation, to the couplings of $\mathrm{W_L}$ (KF = 34) and $\mathrm{W_R}$ (KF = 9900024) in PYTHIA.

2.2 Mixing with the Standard Model W-boson

In a system of two charged vector bosons it is always possible to choose a basis, in which one of the states couples to the SM fermions just like the W-boson predicted in the SM[2]. From now on, we will refer to such a state as $\mathrm{W^{SM}}$. The state orthogonal to $\mathrm{W^{SM}}$, will of course represent our general W'.

$\mathrm{W^{SM}}$ and W' with interactions as in equation (2.1) do not form a mass eigenstate basis in general. Let $\mathfrak{M}_\mathrm{W}^2$ be the charged vector boson mass matrix in this basis $\{\mathrm{W^{SM}}, \mathrm{W}'\}$

$$\mathfrak{M}_\mathrm{W}^2 = \begin{pmatrix} M_{11}^2 & M_{12}^2 \\ M_{12}^2 & M_{22}^2 \end{pmatrix} , \qquad (2.5)$$

then the observed states (mass eigenstates of the Lagrangian) and their masses can be found by diagonalizing the mass matrix squared $\mathfrak{M}_\mathrm{W}^2$. It is easy to see that the mass eigenvalues read

$$M_\ell^2, M_h^2 = \frac{1}{2}\left[M_{11}^2 + M_{22}^2 \mp \sqrt{\left(M_{11}^2 - M_{22}^2\right)^2 + 4\left(M_{12}^2\right)^2}\right] . \qquad (2.6)$$

---

[2]Of course, it is not possible to find such a basis in a general model, but it is possible in each model discussed in this document and in each model trying to predict a state which could be identified with the observed $\mathrm{W^{SM}}$-boson.

Furthermore, the mass eigenstate basis $\{W_\ell, W_h\}$, in which the mass matrix squared has a diagonal form $\mathfrak{M}_W^2 \sim \mathrm{diag}\left(M_\ell^2, M_h^2\right)$, can be obtained by the following rotation

$$\begin{pmatrix} W_\ell \\ W_h \end{pmatrix} = \begin{pmatrix} \cos\xi & \sin\xi \\ -\sin\xi & \cos\xi \end{pmatrix} \begin{pmatrix} W^{\mathrm{SM}} \\ W' \end{pmatrix} , \qquad (2.7)$$

with the so-called mixing angle ξ fulfilling

$$\sin(2\xi) = \frac{2M_{12}^2}{M_\ell^2 - M_h^2} . \qquad (2.8)$$

The observed charged vector boson state is equal to the light eigenstate W_ℓ and W_h denotes the heavy state.

2.3   Extensions of the SM with an enlarged gauge group

One of the steps to the gauge coupling unification in all the Grand Unification Theories of the particle physics is to restore the so-called left-right symmetry. The reason for this is that the left- and right-handed fermions transform differently under the SM's gauge group and in order to be able to unify all the fermions into one representation of a simple group one needs to restore the left-right symmetry during that process. The most popular class of solutions, in this document collectively denoted as left-right symmetric models, is to enlarge the gauge group of the SM by one additional $SU(2)$ group and let the right-handed fermions to transform as doublets under this group, as compared to keeping the singlets of the theory. There exist alternative proposals such as the "alternate" left-right symmetric model [3] in which W' couples to the SM fermions only in pairs with new fermions predicted in this model. Because of the complexity of an extension of PYTHIA needed to incorporate this model, we decided not to include it in this study. The details on the left-right symmetric models can be found in one of the following sections.

There is another thread of extensions of the SM based on an enlarged gauge group which proceeds rather in the opposite direction of the unification process. The motivation for these extensions is that the gauge group of the SM might be only a manifestation of underlying relations between observables in a similar way the strong isospin is manifestation of the mass-scale hierarchy $m_u, m_d \ll \Lambda_{QCD}$. These models can be, based on their couplings to the SM fermions, put into these categories: "-phobic" [4], quark-lepton nonuniversal and generation nonuniversal. The fermiophobic models, in which either couplings to quarks (hadrophobic) or leptons (leptophobic) or both (fermiophobic) vanish cannot be in the leptonic channel at LHC observed, therefore they are not included in our study. The summary of quark-lepton nonuniversal and generation nonuniversal models can be found in the following sections.

Even though, there is no underlying theory predicting exclusively a Sequential Standard Model's (SSM) W'-boson, a copy of SM's W-boson with the difference only in mass, a W'-boson with the couplings to the SM fermions same as the couplings of the SM's W-boson is predicted in both quark-lepton nonuniversal and generation nonuniversal models for certain values of their parameters. As the SSM W' became very popular in the literature, we include it in our numerical analysis.

To summarize, all the models studied in this document can be classified into three categories: (i) left-right symmetric models, (ii) quark-lepton nonuniversal models and (iii) generation nonuniversal models. The following sections contain predictions of a few models within these categories on couplings, mixing angle and mass of the predicted charged vector boson W' together with the

experimental constraints on their parameters. Although most of the existing experimental constraints are out-of-date, it is beyond the scope of this research project to derive constraints based on the latest experimental data. Such a study would definitely offer a very valuable contribution to the search for new resonances at LHC.

2.4 Left-right symmetric (L-R) models

By left-right symmetric models we mean models with one additional $SU(2)$ identified with $SU(2)_R$. Right-handed fermions transform as doublets under $SU(2)_R$ while being singlets under $SU(2)_L$. The situation for the left-handed fermions is reversed. Despite the existence of many specific realisation of this scenario, model-independent low-energy constraints divide these models into several categories: (i) manifest left-right symmetric models, (ii) pseudo-manifest L-R models and (iii) models with no exact left-right symmetry [5].

In the manifest and pseudo-manifest L-R models the, left-right symmetry is exact and thus gauge couplings g_L, g_R corresponding to the $SU(2)_L$, $SU(2)_R$ gauge group are predicted to be both equal to the usual weak gauge coupling g_W. Manifest L-R model furthermore predicts right-handed CKM matrix to be equal to the left-handed one, while equality of CKM matrices up to a diagonal phase matrix in pseudo-manifest model is sufficient.

In the models with no exact left-right symmetry, the left-right symmetry is broken at much higher scale than the $SU(2)_L \times SU(2)_R \times U(1)$-breaking scale and therefore neither the equality of g_L and g_R nor any relationship between the left- and right-handed CKM matrices is required. Further division of models with no exact left-right symmetry according to the predicted right-handed mixing matrix in this document is motivated by the study of low-energy constraints in [5].

Couplings of the predicted purely right-handed W′-boson to the SM fermions together with U_{CKM}^R within different categories of the L-R models can be found in Table 2.1.

The most extensive model-independent study of low-energy constraints on the mass of predicted right-handed charged vector boson and its mixing angle with the $\mathrm{W^{SM}}$-boson was performed already in 1989 by the authors of [5]. Even though this study is outdated, up to our knowledge it is the only model independent study within all the categories of L-R models in the case when the right-handed neutrino is too heavy to be produced in the decay of the right-handed W′. Therefore we include the summary of the low-energy constraints in Tables 2.2 and 2.3.

More recent model-independent constraints were done only for models with light right-handed neutrinos, where by light we mean light enough to be produced in the muon decay. Low-energy constraints from muon decay data and $K_L - K_S$ mass difference (see [6]) are summarized in the Tables 2.4, 2.5.

2.5 Quark-lepton nonuniversal models (Q-LN)

Quark-lepton nonuniversal models, as the name suggests, are defined as models in which W′-boson couples to the quarks with different strength than to the leptons. This is realized by enlarging the gauge group of the SM by one additional $SU(2)$ or eventually another $U(1)$ group. Assuming we added only one $SU(2)$ group and denoting the original $SU(2)_L$ as $SU(2)_q$ and the added one as $SU(2)_l$, left-handed quarks transform as doublets under $SU(2)_q$ while being singlets under $SU(2)_l$. The situation for left-handed leptons is reversed. Right-handed particles are singlets under both $SU(2)_q$ and $SU(2)_l$ and thus the predicted W′ is purely left-handed ($C_{q(l)}^R = 0$).

Table 2.1: List of couplings of W′-boson to the SM fermions and U^R_{CKM}'s within different categories of the L-R models [5]. Here x is the parameter of the model (see low-energy constraints table for available constraints on the mass depending on this parameter), I is the identity matrix and K is a diagonal unitary phase matrix.

Model	Couplings		U^R_{CKM}
	$C^L_{q(l)_{ii}}$	$C^R_{q(l)_{ii}}$	
Manifest L-R	0	1	U^L_{CKM}
Pseudo-manifest L-R	0	1	$U^L_{\mathrm{CKM}} * K$
No L-R 1	0	x	I
No L-R 2	0	x	$\begin{pmatrix} 1 & 0 & 0 \\ 0 & 0 & 1 \\ 0 & 1 & 0 \end{pmatrix}$
No L-R 3	0	x	$\begin{pmatrix} 0 & 1 & 0 \\ 1 & 0 & 0 \\ 0 & 0 & 1 \end{pmatrix}$
No L-R 4	0	x	$\begin{pmatrix} 0 & 1 & 0 \\ 0 & 0 & 1 \\ 1 & 0 & 0 \end{pmatrix}$

Table 2.2: Low-energy constraints on x and $M_{\mathrm{W}'}$ in the L-R models with heavy right-handed neutrinos [5].

Model	$x^2 M^2_{\mathrm{W}}/M^2_{\mathrm{W}'}$	$M_{\mathrm{W}'}/x[\mathrm{GeV}]$
Majorana right-handed neutrino		
(Pseudo-)Manifest L-R	0.0036	1400
No L-R 1	0.0099	810
No L-R 2	0.010	800
No L-R 3	0.015	670
No L-R 4	0.012 [0.032]	740 [450]
Dirac right-handed neutrino		
(Pseudo-)Manifest L-R	0.0036	1400
No L-R 1	0.075	300
No L-R 2	0.032	460
No L-R 3	0.015	670
No L-R 4	0.012 [0.032]	740 [450]

Table 2.3: Low-energy constraints on mixing angle ξ in the L-R models with heavy right-handed neutrinos. Here δ is the phase of either $(U^R_{\text{CKM}})_{ud}$ or $(U^R_{\text{CKM}})_{us}$, for details see [5].

Model	$\xi_g = x\xi$
$\cos\delta = 1$	
(Pseudo-)Manifest L-R	$-0.0020 < \xi_g < 0.0007$
No L-R 1	$-0.0024 < \xi_g < 0.0008$
No L-R 2	$-0.0025 < \xi_g < 0.0007$
No L-R 3	$-0.0014 < \xi_g < 0.0012$
No L-R 4	$-0.0014 < \xi_g < 0.0011$
$\cos\delta = 0$	
(Pseudo-)Manifest L-R	$|\xi_g| < 0.0030$
No L-R 1	$|\xi_g| < 0.013$
No L-R 2	$|\xi_g| < 0.013$
No L-R 3	$|\xi_g| < 0.0045$
No L-R 4	$|\xi_g| < 0.0045$

Table 2.4: Model independent constraints on the mass $M_{W'}$ and mixing angle ξ from muon decay data in the L-R models with light right-handed neutrinos [6]. Letting x vary freely, the best χ^2 is obtained for $x = 0.94 \pm 0.09$ with $M_{W'} \geq 485\text{GeV}$ and $|\xi| \leq 0.0327$.

x	$M_{W'}[\text{GeV}]$	$|\xi|$
0.50	≥ 286	≤ 0.0324
0.75	≥ 379	≤ 0.0321
1.00	≥ 549	≤ 0.0333
1.50	≥ 825	≤ 0.0330
2.00	≥ 1015	≤ 0.0327

Table 2.5: Low-energy constraints on the mass $M_{W'}$ from the K mass difference in the L-R models with light right-handed neutrinos. Here λ_R is the analogue of the Cabibbo angle in the right-handed sector and $\delta_{1,2}$ are CP-violating phases of U^R_{CKM}. For details on these parameters see [6].

Model	$M_{W'}[\text{TeV}]$
(Pseudo-)Manifest L-R	$\left(1.6^{+1.2}_{-0.7}\right)$
No L-R 1,2,3,4	$\cos(\delta_2 - \delta_1)\begin{cases} \geq 0;\ M_{W'} \gtrsim \left(3.4^{+2.5}_{-1.5}\right) x\sqrt{\lambda_R\left(1 - \frac{\lambda_R}{2}\right)\cos(\delta_2 - \delta_1)} \\ < 0;\ M_{W'} \gtrsim \left(2.7^{+2.1}_{-1.2}\right) x\sqrt{-\lambda_R\left(1 - \frac{\lambda_R}{2}\right)\cos(\delta_2 - \delta_1)} \end{cases}$

Table 2.6: Couplings, mass and mixing angle of the charged vector boson predicted in (Q-LN) models. Here M_W is the measured mass of W^{SM} and s, M are the parameters of the model. For the Li-Ma Q-LN model only the best fit values are available, hence this table directly contains the corresponding numerical values for the couplings, mass and the mixing angle.

Model	Couplings		$M_{W'}$	ξ
	$C^L_{q_{ii}}$	$C^L_{l_{ii}}$		
Ununified SM [7], [8]	$\frac{\sqrt{1-s^2}}{s}$	$-\frac{s}{\sqrt{1-s^2}}$	M	$\frac{1}{2}\arcsin\left[\frac{\sqrt{s^2(1-s^2)}(M^2+M_W^2)}{2(M^2-M_W^2)}\right.$ $\left.-\frac{\sqrt{(M^2-M_W^2)^2s^2-(M^2+M_W^2)^2s^4}}{2(M^2-M_W^2)}\right]$
Li, Ma Q-LN [9]	-3.0775	0.32497	1.1715 TeV	-0.62844

Example of what couplings, mass and mixing angle of the predicted charged vector boson read within two different quark-lepton nonuniversal (Q-LN) models can be found in Table 2.6. Details of construction of these models can be found in [7], [8] and [9].

Constraints on the mass and mixing angle of the predicted charged vector boson in Ununified SM from electro-weak precision data are displayed in Figure 2.1. The white part of the plot corresponds to the excluded region and contours represent the dependence of the mixing angle on s^2 and M.

For the Li, Ma Q-LN model only the best fit values of the parameter are available, therefore Table 2.7 contains directly the corresponding numerical values of the couplings, mass and the mixing angle.

2.6 Generation nonuniversality (GN)

In the generation nonuniversal models the gauge group is extended, so that either each or one of the generation of SM left-handed fermions transforms as a doublet under different $SU(2)$ groups and/or singlets under different $U(1)$ groups. The strength of the couplings is thus among different generations different – nonuniversal. Just like in the case of the Q-LN models the predicted W'-boson is purely left-handed.

The predictions for couplings and mixing angle depending on the mass of the W'-boson, parameter t of the Topflavor model and parameters ζ, x, y of the Ma, Li GN models within generation nonuniversal models category are listed in Table 2.7.

Constraints on the mass $M_{W'}$ and t from the electro-weak precission data and from collider searches for the charged vector boson predicted in Topflavor model are displayed in the Figure 2.2. Again, the white part of the plot corresponds to the excluded region and the contours represent the dependence of the mixing angle ξ.

Constraints on the couplings, mixing angle and mass of W' predicted in GNU models from precision electro-weak measurements are displayed in Figures 2.2, 2.3 and 2.4. The first two figures show constraints on $\zeta - 1$ versus x for values $y = 0.1$ and $y = 0.9$. The excluded region of the parameter space on these plots does not actually depend on y, but to show how the mass $M_{W'}$ depend on this parameter, we decided to show the figure for two different values of y. The white part of the plots correspond to the excluded region and the contours represent the mass $M_{W'}$
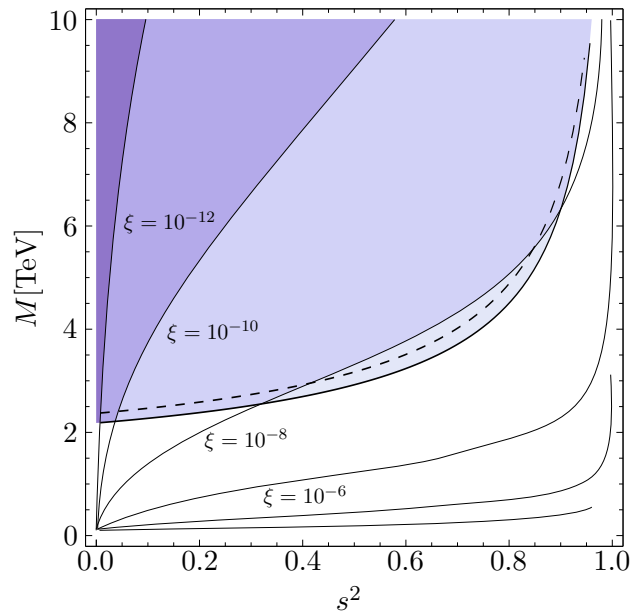
Figure 2.1: Constraints on mass and mixing angle in Ununified SM from electro-weak precision data [8]. The white region of the plot correspond to the excluded parameter space from the electro-weak precision data. The contours represent the dependence of the mixing angle on the mass and s^2.

dependence on the parameters. The other two figures show the exclusion limits on x versus y on two values if $\zeta - 1$. The white part of the plots corresponds as usually to the excluded region, the contours show the dependence of the mixing angle on the parameters.

Table 2.7: Couplings, mass and mixing angle of the charged vector boson predicted in (GN) models. For the exact definitions of parameters y, x and ζ of the Li, Ma GN model and parameter t of the Topflavor model check the reference in the table.

Model	Couplings		$M_{W'}$	ξ
	$C^L_{q(l)_{11,22}}$	$C^L_{q(l)_{33}}$		
Li, Ma GN [10] $\xi = 10^{-12}$ $\xi = 10^{-10}$	$\sqrt{\dfrac{y}{1-y}}$	$-\sqrt{\dfrac{1-y}{y}}$	$\approx M_W \dfrac{1-s_0^2}{1-\sin^2\theta_W}$ $\times \dfrac{1}{(\zeta-1)(1-y)x}$	$\approx \arctan\left[(\zeta-1)y^{\frac{1}{2}}(1-y)^{\frac{3}{2}}\right.$ $\left.\times(1-(x-y)(1-y)^{-1})\right]$
Topflavor [11] $\xi = 10^{-2}$	t	$-t^{-1}$	M	$\dfrac{1}{2}\arcsin\left[\dfrac{(M^2+M_W^2)t}{2(t^2-1)(M^2-M_W^2)}\right.$ $\left.-\dfrac{\sqrt{4M^2M_W^2+(M^2-M_W^2)^2t^2}}{2(t^2-1)(M^2-M_W^2)}\right]$
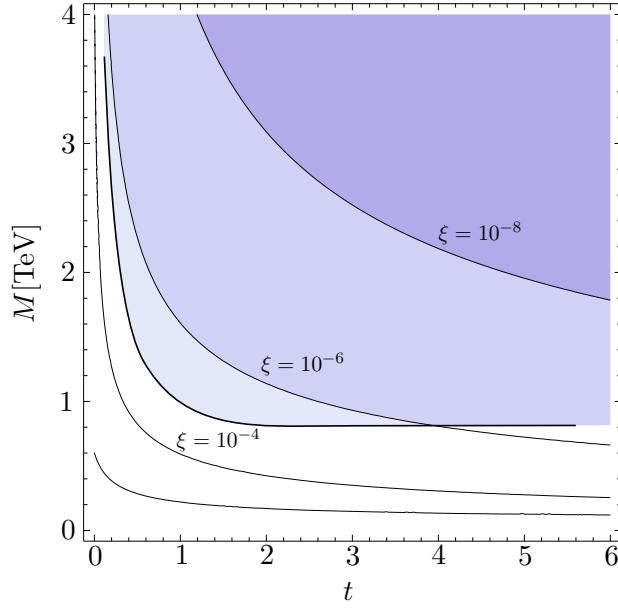
Figure 2.2: Constraints on the mass and mixing angle in Topflavor model from electro-weak precision data and collider searches. The white region of the plot correspond to the excluded parameter space from the electro-weak precision data. Contours represent the dependence of the mixing angle on the mass of the heavy eigenstate and t.
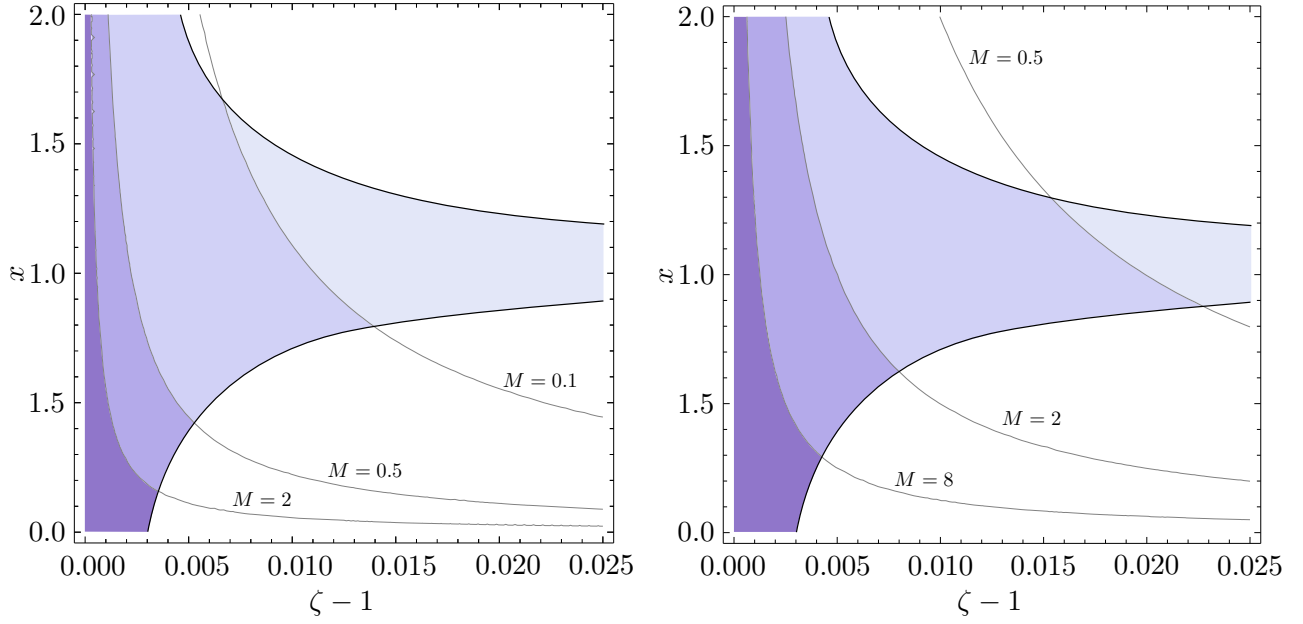
Figure 2.3: Constraints on the parameter space of the Li, Ma GNU model from electro-weak precision data. $\zeta - 1$ versus x exclusion plots for $y = 0.1$ **on the left** and $y = 0.9$ **on the right**. The white part corresponds to the excluded region and the contours represent the dependence of the mass of the heavy eigenstate on the parameters of the model.

Figure 2.4: Constraints on the parameter space of the Li, Ma GNU model from electro-weak precision data. x versus y exclusion plots for $\zeta - 1 = 0.01$ **on the left** and $\zeta - 1 = 0.02$ **on the right**. The white part corresponds to the excluded region and the contours represent the dependence of the mixing angle on the parameters of the model.

12

Chapter 3

Charged vector boson production at hadron colliders

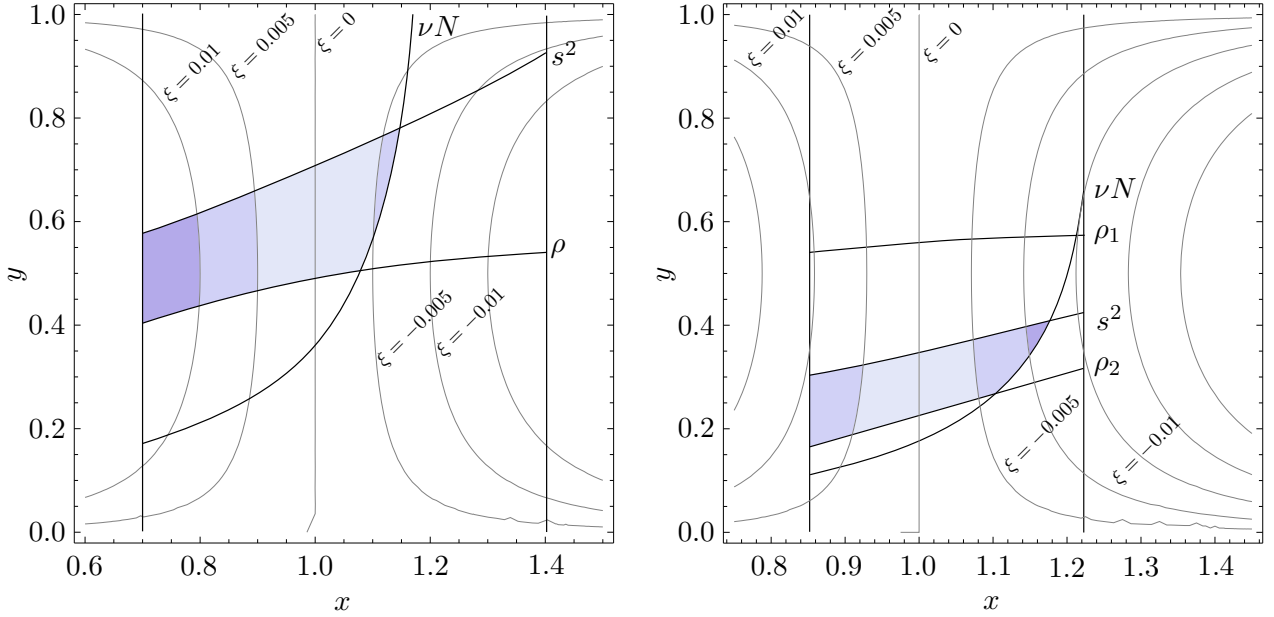In this section we will outline the computation of the differential cross section for the process $q + \overline{q}' \xrightarrow{W^{SM}, W'} \nu + \ell$ taking into account the contributions from the SM vector boson W^{SM} and an additional charged vector boson W'. The leading order Feynman diagram is displayed in Fig. 3.1.
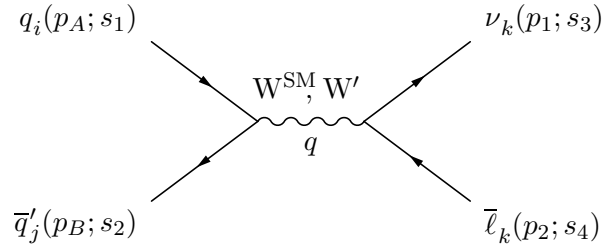
Figure 3.1: $q_i + \overline{q}'_j \xrightarrow{W^{SM}, W'} \nu_k + \overline{\ell}_k$
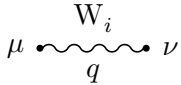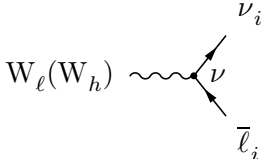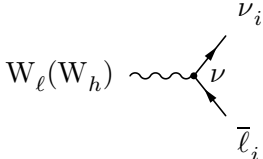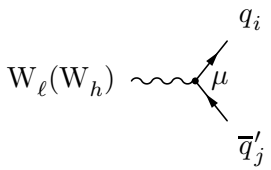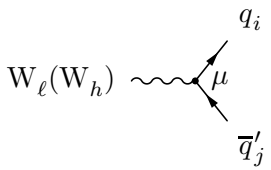
3.1 Feynman rules

The charged-current part of the extension of the SM Lagrangian by an additional W', $\mathcal{L}_{cc} = \mathcal{L}_{cc}^{W^{SM}} + \mathcal{L}_{cc}^{W'}$, can be expressed in the mass eigenstate basis $\{W_\ell, W_h\}$ using Eq. (2.7) (3.1) has been absorbed into the matrices $C_{q(l)_{jk}}$ as defined in Eq. (2.4):

$$\mathcal{L}_{cc} = \frac{g_W}{\sqrt{2}} \left(W_\ell \cos\xi - W_h \sin\xi\right)_\mu \left[\overline{u}_i \gamma^\mu (U_{CKM}^L)_{ij} P_L d_j + \overline{\nu}_j \gamma^\mu P_L e_j\right] + \frac{g_W}{\sqrt{2}} \left(W_\ell \sin\xi + W_h \cos\xi\right)_\mu$$
$$\times \left[\overline{u}_i \gamma^\mu \left((U_{CKM}^L)_{ij} C_{q_{jk}}^L P_L + (U_{CKM}^R)_{ij} C_{q_{jk}}^R P_R\right) d_k + \overline{\nu}_j \gamma^\mu \left(C_{l_{jk}}^L P_L + C_{l_{jk}}^R P_R\right) e_k\right] + \text{h.c.} . \quad (3.1)$$

Collecting the terms proportional to W_ℓ respectively W_h, one can easily read off the Feynman rules for the charged-current interactions of W_ℓ and W_h in a theory with one additional charged vector boson. A summary of the Feynman rules needed for the computation of the cross section of the process $q + \overline{q}' \xrightarrow{W^{SM}, W'} \nu + \ell$ is provided in Table 3.1.

Table 3.1: Feynman rules for $-\mathrm{i}\,\mathcal{M}$ in the SM extension including an additional charged vector boson. Here, $\Gamma_{\ell(h)}$ is the decay rate of $\mathrm{W}_\ell(\mathrm{W}_h)$ and the summation goes only over Greek flavour indices.

External lines (in, out)

Spin $\frac{1}{2}$ (anti)fermion $\qquad$ $u, \bar{u} \quad (v, \bar{v})$

$\mathbf{W}_i$ **propagator** $\qquad \mu \overset{\mathrm{W}_i}{\underset{q}{\sim\!\!\sim}} \nu \qquad$ $\mathrm{i}\left(\dfrac{-g_{\mu\nu}+\frac{q_\mu q_\nu}{M_i^2}}{q^2-M_i^2+\mathrm{i}\,M_i\Gamma_i}\right), \quad (i=\ell,h)$

$\mathbf{W}_\ell$ **vertex** $\qquad \nu_i \qquad -\mathrm{i}\,\gamma^\nu \frac{g_W}{\sqrt{2}}\left[\cos\xi P_L + \sin\xi(C^L_{l_{ii}}P_L + C^R_{l_{ii}}P_R)\right]$

$\mathbf{W}_h$**vertex** $\qquad \mathrm{W}_\ell(\mathrm{W}_h) \quad \nu \quad \bar{\ell}_i \qquad -\mathrm{i}\,\gamma^\nu \frac{g_W}{\sqrt{2}}\left[-\sin\xi P_L + \cos\xi(C^L_{l_{ii}}P_L + C^R_{l_{ii}}P_R)\right]$

$\mathbf{W}_\ell$ **vertex**
$$-\mathrm{i}\,\gamma^\mu \frac{g_W}{\sqrt{2}}\left[\cos\xi(U^L_{\mathrm{CKM}})_{ij}P_L\right.$$
$$\left.+\sin\xi\left((U^L_{\mathrm{CKM}})_{i\alpha}C^L_{q_{\alpha j}}P_L + (U^R_{\mathrm{CKM}})_{i\alpha}C^R_{q_{\alpha j}}P_R\right)\right]$$

$\mathrm{W}_\ell(\mathrm{W}_h) \quad q_i \quad \mu \quad \bar{q}'_j$

$\mathbf{W}_h$**vertex**
$$-\mathrm{i}\,\gamma^\mu \frac{g_W}{\sqrt{2}}\left[-\sin\xi(U^L_{\mathrm{CKM}})_{ij}P_L\right.$$
$$\left.+\cos\xi\left((U^L_{\mathrm{CKM}})_{i\alpha}C^L_{q_{\alpha j}}P_L + (U^R_{\mathrm{CKM}})_{i\alpha}C^R_{q_{\alpha j}}P_R\right)\right]$$

3.2   Matrix element squared

In order to describe the kinematics of the matrix element squared we introduce the usual Mandelstam variables which are defined as follows:

$$s = (p_A + p_B)^2 \ , t = (p_A - p_1)^2 = (p_B - p_2)^2 \ , u = (p_A - p_2)^2 = (p_B - p_1)^2 \ . \tag{3.2}$$

Using the Feynman rules listed in Tab. 3.1, the matrix elements for the individual amplitudes, either with W_ℓ or W_h, can be written as:

$$\mathcal{M}^{\mathrm{W}_\ell}_{ijk} = \frac{g_W^2}{2}\bar{v}(p_B; s_2)\gamma^\mu\left[\cos\xi(U^L_{\mathrm{CKM}})_{ij}P_L + \sin\xi\left((U^L_{\mathrm{CKM}})_{i\alpha}C^L_{q_{\alpha j}}P_L + (U^R_{\mathrm{CKM}})_{i\alpha}C^R_{q_{\alpha j}}P_R\right)\right]u(p_A; s_1)$$

$$\times\left(\frac{-g_{\mu\nu}+\frac{q_\mu q_\nu}{M_\ell^2}}{q^2 - M_\ell^2 + \mathrm{i}\,M_\ell\Gamma_\ell}\right)\bar{u}(p_1; s_3)\gamma^\nu\left[\cos\xi P_L + \sin\xi(C^L_{l_{kk}}P_L + C^R_{l_{kk}}P_R)\right]v(p_2; s_4) \ , \tag{3.3}$$

$$
\mathcal{M}^{\mathrm{W}_h}_{ijk} = \frac{g_W^2}{2} \bar{v}(p_B; s_2) \gamma^\mu \left[-\sin\xi (U^L_{\mathrm{CKM}})_{ij} P_L + \cos\xi \left((U^L_{\mathrm{CKM}})_{i\alpha} C^L_{q_{\alpha j}} P_L + (U^R_{\mathrm{CKM}})_{i\alpha} C^R_{q_{\alpha j}} P_R \right) \right] u(p_A; s_1)
$$

$$
\times \left(\frac{-g_{\mu\nu} + \frac{q_\mu q_\nu}{M_h^2}}{q^2 - M_h^2 + \mathrm{i}\, M_h \Gamma_h} \right) \bar{u}(p_1; s_3) \gamma^\nu \left[-\sin\xi P_L + \cos\xi (C^L_{l_{kk}} P_L + C^R_{l_{kk}} P_R) \right] v(p_2; s_4) \ , \quad (3.4)
$$

where i, j, k are flavor indices of quarks and leptons in the mass eigenstate basis and Greek flavor indices are summed over implicitly.

From the expressions above, it is easy to compose the full spin- and color-averaged matrix element squared:

$$
\begin{aligned}
\overline{\sum} |\mathcal{M}|^2_{ijk} &= \overline{\sum} \left(\mathcal{M}^{\mathrm{W}_\ell}_{ijk} + \mathcal{M}^{\mathrm{W}_h}_{ijk} \right) \left(\mathcal{M}^{\mathrm{W}_\ell}_{ijk} + \mathcal{M}^{\mathrm{W}_h}_{ijk} \right)^* \\
&= \overline{\sum} \left(|\mathcal{M}^{\mathrm{W}_\ell}|^2 + |\mathcal{M}^{\mathrm{W}_h}|^2 + 2\Re(\mathcal{M}^{\mathrm{W}_\ell})^* \mathcal{M}^{\mathrm{W}_h} \right)_{ijk} \ .
\end{aligned}
\quad (3.5)
$$

The final expression for the spin- and color-averaged matrix element squared is a little bit too long to be written down explicitly. However, since the processes with either left- or right-handed neutrinos in the final state have to be distinguished in `PYTHIA`, because of the mass of the right-handed neutrino, we actually need only the expressions for the corresponding matrix elements squared.

Let us denote $\mathcal{M}^{L(R)}$ the matrix element for the process with left-(right-)handed neutrino in the final state, then one can write:

$$
\begin{aligned}
\overline{\sum} |\mathcal{M}^L|^2 &= \frac{g_W^4}{4N_c} t^2 \left\{ \left(1 - \frac{1}{2}\sin^2 2\xi \right) \left(\frac{A^2}{D_\ell^2} + \frac{B_L^2 C_L^2}{D_h^2} \right) + I \Big[A B_L C_L \right. & (3.6) \\
&\quad + \frac{1}{4}\sin^2 2\xi \left(A^2 - B_L^2 + B_L^2 C_L^2 + A^2 C_L^2 - 2 A B_L C_L \right) & (3.7) \\
&\quad \left. + \frac{1}{2}\sin 4\xi \left(B_L^2 C_L + A B_L C_L^2 - A B_L - A^2 C_L \right) \Big] \right\} \ ,
\end{aligned}
$$

$$
\overline{\sum} |\mathcal{M}^R|^2 = \frac{g_W^4}{4N_c} (t^2 + t m_\nu^2) \left\{ \left(1 - \frac{1}{2}\sin^2 2\xi \right) \frac{B_R^2 C_R^2}{D_h^2} + \frac{1}{4} I \sin^2 2\xi B_R^2 C_R^2 \right\} \ , \quad (3.8)
$$

where the flavor indices i, j, k were suppressed. N_c stands for number of colors, the Mandelstam variables have been defined in Eq. (3.2) and quantities D_ℓ^2, D_h^2, I and A, B, C were defined as

$$
\begin{aligned}
D_{\ell(h)}^2 &\equiv (s - M_{\ell(h)}^2)^2 + M_{\ell(h)}^2 \Gamma_{\ell(h)}^2 \ , & (3.9\mathrm{a}) \\
I &\equiv \frac{(s - M_\ell^2)(s - M_h^2) + M_\ell M_h \Gamma_\ell \Gamma_h}{D_\ell^2 D_h^2} \ , & (3.9\mathrm{b}) \\
A_{ij} &\equiv (U^L_{\mathrm{CKM}})_{ij} \ , & (3.9\mathrm{c}) \\
(B_{L(R)})_{ij} &\equiv (U^{L(R)}_{\mathrm{CKM}})_{i\alpha} C^{L(R)}_{q_{\alpha j}} \ , & (3.9\mathrm{d}) \\
(C_{L(R)})_k &\equiv C^{L(R)}_{l_{kk}} \ . & (3.9\mathrm{e})
\end{aligned}
$$

The summation in the formulas above goes only over Greek flavor indices.

Masses of incoming states as well as the mass of outgoing charged lepton were assumed to be negligible compared to the masses M_ℓ and M_h and couplings $C_q^{L(R)}$ and $C_l^{L(R)}$ were for simplicity assumed to be real[1].

The reason why the mass of neutrino is not considered to be negligible in general, is that the couplings of W′ to the right-handed fermions are kept non-zero, as compared to the W$^{\mathrm{SM}}$ which couples only to the left-handed fermions. Therefore, in general a right-handed neutrino whose mass is usually assumed to be very large to allow for See-Saw mechanism of neutrino masses, can be one of the final states of this process.

It is interesting to note, that in the presence of mixing i.e. $\xi \neq 0$, the interference term survives even in the case of a purely right-handed W′. The reason is, that once you allow for mixing the light mass eigenstate W$_\ell$, identified with the observed W-boson, develops a non-zero right-handed component.

All the previous discussion as well as the discussion following in the next section, contains formulas for positively charged vector bosons (as is clear from Figure 3.1). The expressions for the matrix elements squared and the cross sections for negatively charged vector bosons can be simply obtained by the exchange of Mandelstam variables t and u.

3.3 Differential partonic cross section

Following the discussion in [12], the differential cross section of a $2 \to 2$ process can be written as:

$$d\hat{\sigma} = \frac{\overline{\sum|\mathcal{M}|^2}}{F}dQ, \tag{3.10}$$

where dQ is the Lorentz invariant phase space factor

$$dQ = (2\pi)^4 \delta^4(p_1 + p_2 - p_A - p_B)\frac{d^3p_1}{(2\pi)^3 2E_1}\frac{d^3p_2}{(2\pi)^3 2E_2} , \tag{3.11}$$

and the incident flux in the laboratory is for a general collinear collision between A and B

$$F = |\mathbf{v}_A - \mathbf{v}_B|2E_A 2E_B = 4\left((p_A \cdot p_B)^2 - m_A^2 m_B^2\right)^{1/2} . \tag{3.12}$$

In the limit of massless incoming states the incident flux can be written as

$$F = 2s , \tag{3.13}$$

and the phase space element in the center-of-mass frame reads:

$$dQ = \frac{1}{4\pi^2}\frac{|\mathbf{p}_1|}{4\sqrt{s}}d\Omega_{\mathrm{CM}} = \frac{1}{8\pi s}dt . \tag{3.14}$$

Thus the differential cross section in the center-of-mass frame in the limit of massless incoming states can be written as:

$$d\hat{\sigma} = \frac{1}{32\pi^2}\frac{|\mathbf{p}_1|}{s^{3/2}}\overline{\sum|\mathcal{M}|^2}d\Omega_{\mathrm{CM}} = \frac{1}{16\pi s^2}\overline{\sum|\mathcal{M}|^2}dt . \tag{3.15}$$

---

[1]This simplification is allowed within all models under study in this document.

The differential partonic cross sections for the processes with matrix elements $\mathcal{M}^L$ and $\mathcal{M}^R$ can be using the formulas above written as

$$d\hat{\sigma}_{ijk}^{L(R)} = \frac{g_W^4}{16\pi s^2} \overline{\sum} |\mathcal{M}^{L(R)}|_{ijk}^2 dt \ . \tag{3.16}$$

Implementing a process in PYTHIA practically means typing-in the expressions for $\frac{s^2}{\pi}\frac{d\hat{\sigma}}{dt}$ [1]. Therefore, let us take a look at the expression for the individual processes 493–498 (check the next section for the table of new processes implemented in PYTHIA):

$$\frac{s^2}{\pi}\frac{d\hat{\sigma}^{492+k}}{dt} = \frac{1}{4}\frac{\alpha_{\text{em}}}{\sin^4\theta_W} \sum_{i,j} \overline{\sum} |\mathcal{M}^L|_{ijk}^2 \Big|_{N_c=3}, \quad \frac{s^2}{\pi}\frac{d\hat{\sigma}^{494+k}}{dt} = \frac{1}{4}\frac{\alpha_{\text{em}}}{\sin^4\theta_W} \sum_{i,j} \overline{\sum} |\mathcal{M}^R|_{ijk}^2 \Big|_{N_c=3},$$

$$\tag{3.17}$$

where we have used $g_W^4 = \frac{16\pi^2\alpha_{\text{em}}^2}{\sin^4\theta_W}$. The sum over flavor indices i, j goes through all allowed combinations of quarks[2] and $k = 1, 2, 3$ denotes flavor of outgoing leptonic states.

---

[2]So that either the positively or negatively charged vector boson is produced.

Chapter 4

Implementation in the Monte Carlo generator

As briefly mentioned in Section 2.1, `PYTHIA` (in version 6.4.20) contains two particles with W'-like behaviour. One of them is W_L, in original `PYTHIA` notation W', with flavour code (`KF`) 34. It can be produced e.g. in the process $f + \overline{f}' \rightarrow W_L$ with id (`ISUB`) 142. Decay is handled automatically and the individual decay channels can be switched on or off on demand. The other particle W_R with `KF` = 9900024 can be produced e.g. in the process $f + \overline{f}' \rightarrow W_R$ with `ISUB` = 354. In principle, therefore, it is possible to simulate the production of a general W' and its consequent decay at Large Hadron Collider (LHC). However, in the original `PYTHIA` code, the interference of W_L with W^{SM} is not implemented, neither is there a possibility for user to choose U^R_{CKM} or generation non-universal of couplings of either W_L or W_R to the fermions of SM and thus, in order to be able to perform serious studies of W' discovery at LHC we decided to extend `PYTHIA`.

Since the channel $l + \not{E}_T$ will be straightforward to observe and at LHC will be one of the first channels to be analysed, we have chosen to extend `PYTHIA` to the implement processes $q + \overline{q}' \overset{W^{SM},W'}{\longrightarrow} \nu + \ell$ accounting for mixing of W_L, W_R and interference of the corresponding mass eigenstates. Furthermore W_R was generalized so that user chosen U^R_{CKM} and $C^{V(A),W_R}_{q(l)}$ can be specified, as compared to the fixed coupling $C^{V(A),W_R}_{q(l)} = C^{V(A),W^{SM}}_{q(l)}$ and the fixed CKM matrix $U^R_{CKM} = U^L_{CKM}$ assumption in the original version of `PYTHIA`.

The following section describes a short summary on how to extend `PYTHIA` and a brief user's manual for the extension offered in this document.

4.1 Extending `PYTHIA`

In order to implement a new process in `PYTHIA` a few basic steps are required. As described in [1], for each process one wants to include, `ISUB` which is not in use has to be picked and after setting the name of the process in `PROC(ISUB)` one needs to specify the type of the process and its massive final states in `ISET(ISUB)` and `KFPR(ISUB,1:2)`. The expressions for matrix elements are then typed into the subroutine `PYSIGH` and the final state selection code in the subroutine `PYSCAT`. For processes with an implicit resonance in the cross section the subroutines `PYRAND`, `PYMAXI` need to be altered.

The list of new processes offered in this extension can be found in Table 4.1. The exact formulae for differential partonic cross sections coded in `PYTHIA` can be found in Section 3.2.

Table 4.1: New processes implemented in PYTHIA. All the processes account for mixing and inter-ference of W^{SM} (KF = 24) and $W' = W_R$(KF = 34) $+ W_L$(KF = 9900024).

ISUB	Process
492	$q + \overline{q}' \rightarrow \nu_e + e$ (W/W')
493	$q + \overline{q}' \rightarrow \nu_\mu + \mu$ (W/W')
494	$q + \overline{q}' \rightarrow \nu_\tau + \tau$ (W/W')
495	$q + \overline{q}' \rightarrow (\nu_R)_e + e$ (W/W')
496	$q + \overline{q}' \rightarrow (\nu_R)_\mu + \mu$ (W/W')
497	$q + \overline{q}' \rightarrow (\nu_R)_\tau + \tau$ (W/W')

To make place for all additional features offered in the extension, we have decided to change the length of the array PARU from 200 to 230 and the list of all the entries of this array playing role in our extension together with the explanation of their purpose and their default values is contained in the following section. Furthermore, three entries of array MSTU were reserved for switches used in the cross section computation routines for new implemented processes (see following section).

As the PYTHIA code is contained in a single file, all the code of this extension had to be included in this file as well. For diff of the original PYTHIA code (version 6.4.20) and code containing the extension, please contact the corresponding author.

4.2 Details on the simulation

All the new implemented processes together with their ISUB numbers can be found in Table 4.1. For details and examples on the use of PYTHIA discuss the original manual [1].

```
COMMON/PYDAT1/MSTU(200),PARU(230),MSTJ(200),PARJ(200)
```

MSTP(197) (D = 0) to specify that the mass and width of either W_L (KF = 34) or W_R (KF = 9900024) should be used in the formulas for cross section of processes 493-498

   = 0 : mass and decay rate of W_L (KF = 34) will be used in the propagator of the heavy mass eigenstate in processes 493-498

   = 1 : mass and decay rate of W_R (KF = 9900024) will be used in the propagator of the heavy mass eigenstate in processes 493-498

MSTP(198) (D = 0)

   = 0 : couplings of W_L (KF = 34) to the third generation of SM fermions will be taken to be equal to the couplings to the first and second generation

   = 1 : couplings to the third generation are taken from PARU(137:140)

MSTP(199) (D = 0)

   = 0 : couplings of W_R (KF = 9900024) to the third generation of SM fermions will be taken to be equal to the couplings to the first and second generation

   = 1 : couplings to the third generation are taken from PARU(137:140)

MSTP(200) (D = 0) a switch on which part of the cross section will be computed

   = 0 : $W^{SM} + W' +$ interference

   = 1 : only W^{SM}

   = 2 : only W'

19

```
= 3 :      only interference
= 4 :      W′ + interference
```
Note: for D = 3, 4 – possibility of negative cross section warning.

`PARU(131)` – `PARU(134)` : couplings of a W_L (`KF = 34`) to the first and second generation of SM fermions; default values are equal to the couplings of W^{SM} (`KF = 24`).

`PARU(131)`, `PARU(132)` : (D = 1., −1.) vector and axial couplings of the first and second generation quark–antiquark pair to W_L.

`PARU(133)`, `PARU(134)` : (D = 1., −1.) vector and axial couplings of the first and second generation lepton–neutrino pair to W_L.

`PARU(137)` – `PARU(140)` : couplings of a W_L (`KF = 34`) to the third generation of SM fermions.

`PARU(137)`, `PARU(138)` : (D = 1., −1.) vector and axial couplings of the third generation quark–antiquark pair to W_L.

`PARU(139)`, `PARU(140)` : (D = 1., −1.) vector and axial couplings of the third generation lepton-neutrino pair to W_L.

`PARU(201)` – `PARU(204)` : couplings of a W_R (`KF = 9900024`) to the first and second generation of SM fermions; default values are in absolute value equal to the couplings of W^{SM} (`KF = 24`), so that W_R is purely right-handed

`PARU(201)`, `PARU(202)` : (D = 1., 1.) vector and axial couplings of the first and second generation quark–antiquark pair to W_R.

`PARU(203)`, `PARU(204)` : (D = 1., 1.) vector and axial couplings of the first and second generation lepton–neutrino pair to W_R.

`PARU(207)` – `PARU(210)` : couplings of a W_R (`KF = 9900024`) to the third generation of SM fermions.

`PARU(207)`, `PARU(208)` : (D = 1., −1.) vector and axial couplings of the third generation quark–antiquark pair to W_R.

`PARU(209)`, `PARU(210)` : (D = 1., −1.) vector and axial couplings of the third generation lepton–neutrino pair to W_R.

`PARU(211)` – `PARU(219)` : real part of U^R_{CKM}

`PARU(211)`, `PARU(213)` : (D = 1., 0., 0.) first row of the real part of U^R_{CKM}

`PARU(214)`, `PARU(216)` : (D = 0., 1., 0.) second row of the real part of U^R_{CKM}

`PARU(217)`, `PARU(219)` : (D = 0., 0., 1.) third row of the real part of U^R_{CKM}

`PARU(220)` – `PARU(228)` : imaginary part of U^R_{CKM}

`PARU(220)`, `PARU(222)` : (D = 0., 0., 0.) first row of the imaginary part of U^R_{CKM}

`PARU(223)`, `PARU(225)` : (D = 0., 0., 0.) second row of the imaginary part of U^R_{CKM}

`PARU(226)`, `PARU(228)` : (D = 0., 0., 0.) third row of the imaginary part of U^R_{CKM}

`PARU(229)` : mixing angle of $W' = W_L$(`KF = 34`) $+ W_L$(`KF = 9900024`) with W^{SM} (`KF = 24`)

Chapter 5

Numerical results

For all the numerical computations in this chapter we have used the general purpose Monte Carlo generator `PYTHIA` (version 6.4.20) with an extension described in the previous chapters. During the M2 PSA internship we did not have enough time for a systematic numerical analysis of the dependences of the signal characteristics on all the parameters of the models discussed in Chapter 2. However, to show the main features of all the models we did a comparison of the transverse mass distributions and charge asymmetries for one point in the parameter space for each model. The results of our main numerical analysis can be found in Section 5.4.

To make sure, that the W′-boson with the values of the parameters chosen for the main analysis will be observable at the LHC we did also an estimation of the total cross section of the process $q + \overline{q}' \xrightarrow{\text{W}'} \nu + \ell$ as a function of the mass of the heavy eigenstate M_h. Furthermore, to see what is the total decay rate around the values of the parameters chosen for the main analysis, we computed the total decay rate of the W_h as a function of the parameters which directly influence the couplings of the W′ for fixed mass of $M_h = 800$ GeV.

The second section of this chapter is devoted to a comparison of the transverse mass distribution obtained with `PYTHIA`'s original implementation of $q + \overline{q}' \xrightarrow{\text{W}^{\text{SM}}, \text{W}'} \nu + \ell$ with the transverse mass distribution obtained with our enhanced implementation accounting for the interference between the corresponding mass eigenstates.

Before discussing all the numerical results of this section, let's have a brief look at what the transverse mass distribution and charge asymmetry exactly are.

5.1 Transverse mass and charge asymmetry

In the rest frame of a decaying charged vector boson W, the energy of the charged lepton is simply $M_W/2$. This fact can be used to make precision measurements of the mass of the W. The transverse momentum p_{T_ℓ} distribution of the outgoing charged lepton will be strongly peaked at $M_W/2$ [13]:

$$\frac{1}{\sigma}\frac{d\sigma}{dp_{T_\ell}} \sim \left(1 - \frac{4p_{T_\ell}^2}{M_W^2}\right)^{-\frac{1}{2}} . \tag{5.1}$$

However, the square-root singularity of the distribution is somewhat smeared out by the finite width and non-zero transverse momentum of the W-boson. Therefore, for precision measurements of the mass it is more suitable to use the transverse mass distribution of the W-boson, where the

21

transverse mass is defined as:

$$M_T^2 = 2|p_{T_\ell}||p_{T_{\nu_\ell}}|(1 - cos\Delta\phi_{\ell\nu_\ell}) , \tag{5.2}$$

with $\Delta\phi_{\ell\nu_\ell}$ being the angle between the outgoing charged lepton and its corresponding neutrino. The reason is that the information from the missing transverse momentum of the W-boson is taken into account further sharpening the peak. At leading order, in the case of negligible mass of the neutrino and in the absence of any quark transverse momentum the transverse mass can be estimated by $M_T = 2|p_{T_l}|$ and therefore has a peak at $M_T = M_W$. In a system of two charged vector bosons, the transverse mass distribution will have two peaks at both masses of the mass eigenstates.

Another interesting characteristics of the charged vector boson production and its consequent decay into the leptonic channel is the charge asymmetry. The main partonic channel contributing to the W^+-boson production at the LHC is the u $\overline{d}$ channel while the main channel for the W^- production is the $\overline{u}$ d channel. Since the u $\overline{d}$ parton luminosity will be bigger then the $\overline{u}$ d parton luminosity there will be an asymmetry concerning the production of a $W^+ - boson$ resp. a $W^- - boson$. Charge asymmetry defined as:

$$A_W(y) = \frac{d\sigma(W^+)/dy - d\sigma(W^-)/dy}{d\sigma(W^+)/dy + d\sigma(W^-)/dy} \tag{5.3}$$

therefore, provides a measure of the relative shape of the u and d quark distributions. Unfortunately the rapidity of charged vector bosons is difficult to measure accurately because of the undetected neutrino in the final state. What can be measured with high precision is the closely related charged lepton asymmetry $A_\ell(y)$:

$$A_\ell(y) = \frac{d\sigma(\overline{\ell})/dy - d\sigma(\ell)/dy}{d\sigma(\overline{\ell})/dy + d\sigma(\ell)/dy} . \tag{5.4}$$

Both transverse mass distributions and charge asymmetries for different models discussed in Chapter 2 are shown in Section 5.4.

5.2 The effects of the interference

To show the effect of the interference as well as to compare our implementation of the process $q + \overline{q}' \overset{\mathrm{W^{SM},W'}}{\longrightarrow} \nu + \ell$ with the original implementation in `PYTHIA` we performed two simulations. In the first simulation we have used the processes `ISUB` $= 2, 142$ for the production of $\mathrm{W^{SM}}$ and W' and allowed their automatic decay into an electron and its corresponding neutrino. For the second simulation we have used the process `ISUB` $= 493$ from our extension. In both simulations the couplings of the W' were set to be equal to the couplings of the $\mathrm{W^{SM}}$, thus simulating the W'-boson in the Sequential Standard Model. The mixing angle relevant for the process 493 was set to zero and the mass of the W'-boson was chosen to be $M_{\mathrm{W}'} = 500$ GeV, what should be small enough to make the effect of the interference clearly observable.

Furthermore, since the original implementation is based on a $2 \to 1$ process as compared to the $2 \to 2$ implementation in our extension, the scale for the evaluation of the parton distribution functions in the process 493 needed to be set to the usual scale used in $2 \to 1$ processes for a meaningful comparison. Because of the time limitations both simulations were performed without the initial and final state radiation. However, these should not be important for the demonstration of the effects of the interference. As the event selection criteria we have used the transverse

momentum cut $p_{T_\ell} > 20$ GeV and the rapidity cut $|y_\ell| < 2.4$. The transverse mass distribution of the production of W^{SM}, W' and their consecutive decays into the leptonic channel with and without the interference between W^{SM} and W' are displayed in Figure 5.1.
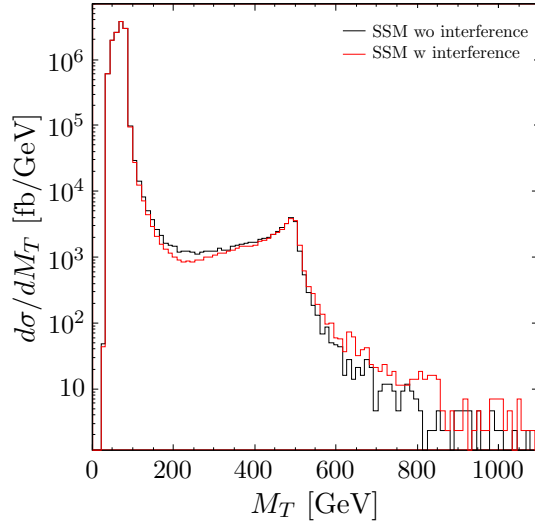
PSfrag replacements

Figure 5.1: Comparison of the transverse mass distribution of the W' in the Sequential Standard Model produced with the original `PYTHIA` code (without interference) and the transverse mass distribution of the same W'-boson with the extended `PYTHIA` code to account for the interference.

The transverse mass distribution has in both cases two sharp peaks at the masses of the W^{SM} and W' and since both interaction states W^{SM} and W' are purely left-handed, the effect of the interference should be nicely observable and indeed the destructive interference in the area between the peaks and the constructive interference on the right side of the W' peak of the transverse mass distribution are obvious. More details on the importance of the effect of interference for determination of the helicities of the couplings of W'-boson can be found in [14].

5.3   Total cross section and W'-boson decay rate

The estimate of the total cross sections of the processes $q + \overline{q}' \xrightarrow{W'} \nu + \ell$ as well as the total decay rate of the heavy mass eigenstate W_h within the models discussed in Chapter 2 were done using `PYTHIA` as well. For the evaluation of the total cross section the process 493 was used with the contributions from W^{SM} and the interference part of the formula for the cross section switched off. The widths of all the particles in `PYTHIA` are computed before the initialization of the simulation and the widths of W_L and W_R were extracted from the table of total decay rates and branching ratios offered by `PYTHIA`.

It is important to note that the values of the total cross sections as well as the total decay rates present only rough estimates of the physical values since in reality the total cross section for the W' cannot be disentangled from the total cross section of the combined process and the decay rates of the W_L and W_R are not the actual decay rates of the physical mass eigenstates in the presence of non-zero mixing.
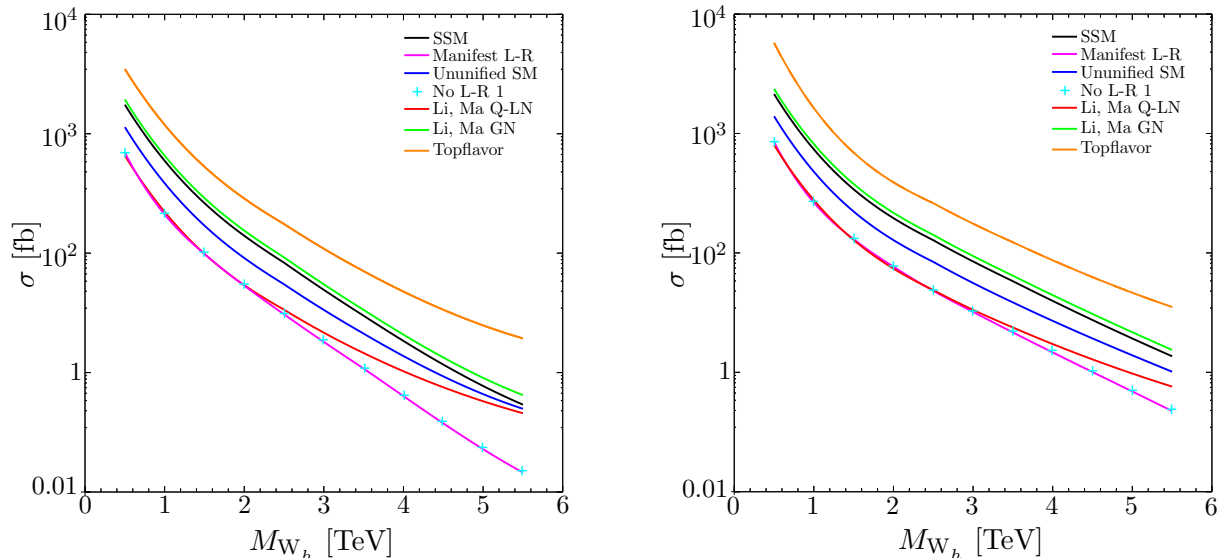
Figure 5.2: Total cross section of $q + \overline{q}' \xrightarrow{\mathrm{w}'} \nu + \ell$ in all the models included in the main numerical study as a function of the mass of the heavy mass eigenstate. Curves in the plot **on the left** represent the low luminosity period with the center of mass energy of 10 TeV, curves in the plot **on the right** the high luminosity period at 14 TeV.

The dependence of the total cross section on the mass of the heavy eigenstate W_h for all the studied models is displayed in Figure 5.2. For the models where more then one point of the parameter space was available for the study, we show the dependence of the total decay rate on the model-parameters in Figure 5.3.

The summary of the parameters of different models used in this numerical analysis (applicable in the following section as well) can be found in Table 5.1.

From the dependence of the total cross section of the process $q + \overline{q}' \xrightarrow{\mathrm{w}'} \nu + \ell$, it is obvious that for the masses of the heavy eigenstate of the system W^{SM}, W' below 3 TeV the values of the cross sections are well above the discovery limits in the low luminosity period of LHC ($L \approx 10\ \mathrm{fb}^{-1}$) as well as in the high luminosity period ($L \approx 300\ \mathrm{fb}^{-1}$).

5.4 Signal characteristics

As discussed in Section 5.1, there are two particularly interesting characteristics worth investigating. In this section we offer both the transverse mass distribution and the charge asymmetry extracted from the simulations of a reasonable set of the processes discussed in Chapter 2 for chosen values of their parameters (see Table 5.1) with the electron and its neutrino in the final state. This time, in order to get better statistics, we set the hardwired kinematic cut on the center of mass energy at 350 GeV, while as the selection criteria for the final states same cuts on p_{T_e} and y_e as in the section 5.2 were applied. The mass of the heavy eigenstate W_h was set to 800 GeV and the center of mass energy to 10 TeV. The generation of the distributions within all the models under study and the generation of the signal without W'-boson was done using the process 493.

Both, the transverse mass distribution and the charge asymmetry as a function of an outgoing

Table 5.1: List of values of the parameters of all the models used in the total cross section and total decay rate estimates and in the main numerical analysis. The mass of the W'-boson was always set to 800 GeV.

Manifest L-R	$U^R_{\mathrm{CKM}} = U^L_{\mathrm{CKM}}$
	$m_{\nu_R} = 0$
No L-R 1	$U^R_{\mathrm{CKM}} = I$
	$x = 0.5$
	$m_{\nu_R} = 0$
Ununified SM	$s^2 = 0.25$
Li, Ma Q-LN	$C^L_{q_{ii}} \left(\frac{g_W}{\sqrt{2}}\right)^{-1} = -3.0775$
	$C^L_{l_{ii}} \left(\frac{g_W}{\sqrt{2}}\right)^{-1} = 0.32497$
Li, Ma GN	$y^2 = 0.55$
Topflavor	$t = 2$

charged lepton rapidity are shown in Figure 5.4. The "SM" label in both figure denotes the signal without W'-boson.

Both figures show very interesting signals for the transverse mass above 400 GeV as compared to the signal without the presence of an additional charged vector boson. The transverse mass distribution in particular nicely shows the effects of the interference, where all the models with a purely left-handed W'-boson start below the tail from the W^{SM}-boson (see the curve denoted as "SM"), while both models with a purely right-handed W'-boson start above it. It is important to note, that the difference in the width of the individual W'-bosons predicted in different models has a large impact on the transverse mass distribution.

The charge asymmetry also shows significantly different shapes for all the models containing a W'-boson as compared to the signal without it. The difference between the signals with and without the W'-boson is due to the different ranges of x values probed, as they are closely related to the masses of W^{SM}-boson and W'-boson. The minute differences between the signals in models with W'-boson are, apart from the different couplings of the W'-boson, mainly caused by the width of the W'-boson and are probably too small to be used to discriminate the models in the early LHC data. Therefore, the shapes of some other distributions and/or asymmetries should be investigated.

For the left-right symmetric models, angle distribution of the outgoing charged lepton and the forward-backward asymmetry derived from it should show more significant differences in comparison with models predicting a purely left-handed W'-boson. To distinguish the generation nonuniversal models, it would be worthwhile to compare the transverse mass distributions and charge asymmetries for different generations of quarks and leptons in the final state. In particular, the $e\nu_e$ channel versus the $\tau\nu_\tau$ channel as well as tb channel versus the light jets in the final state should be compared. The tb channel can also serve for distinguishing the left-right symmetric models with heavy right-handed neutrinos.

Concerning the "-phobic" models, different channel from the leptonic one needs to be included in the study in order to observe any signal at all. For leptophobic models, quarks in the final state

especially the tb channel should be investigated, as the couplings of the W′-boson to the lepton within these models vanish completely. For fermiophobic models, in which the W′-boson does not couple to the SM fermions at all, final state like WZ could be useful.
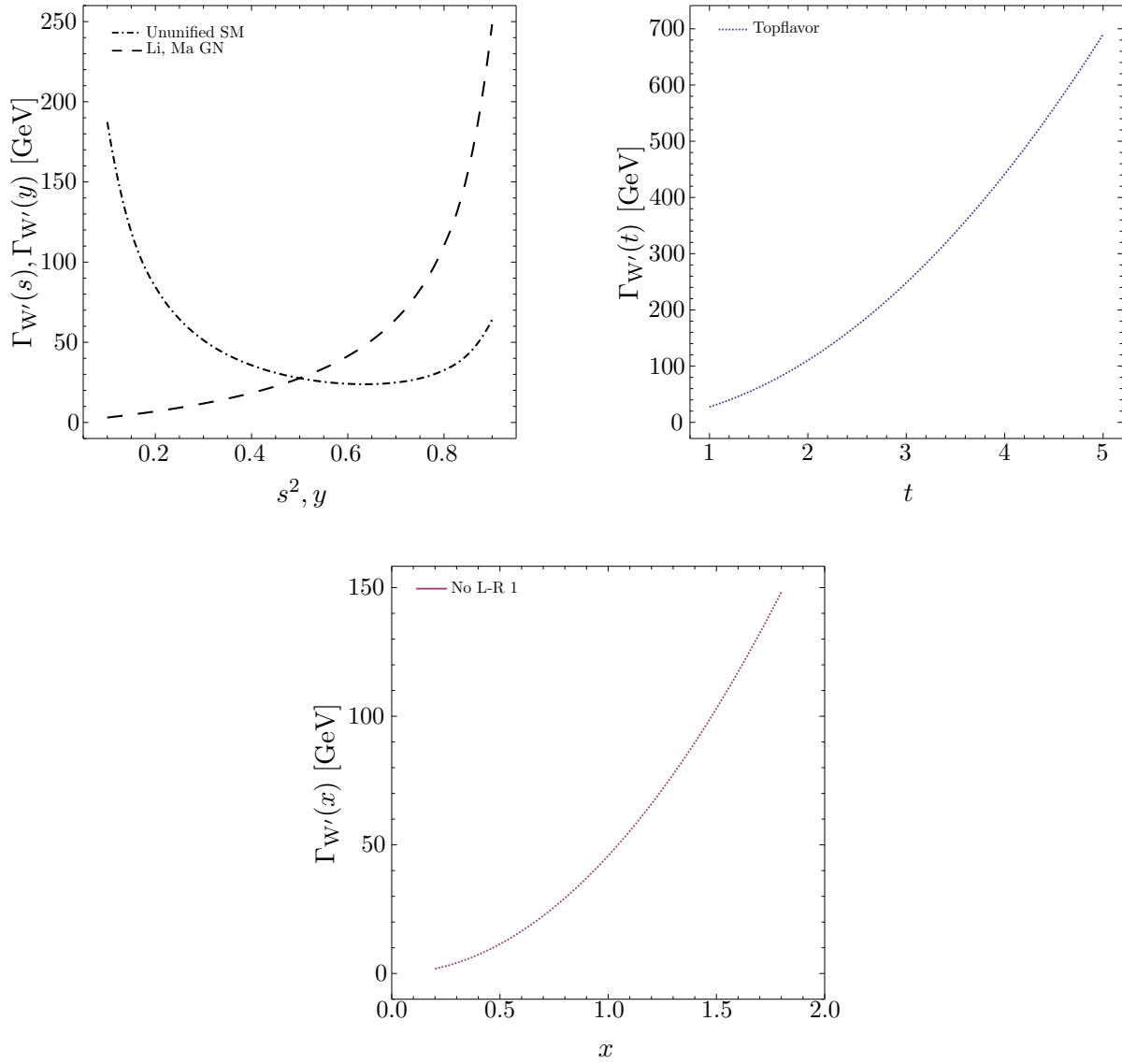
Figure 5.3: Total decay rate of W'-boson with mass 800 GeV as a function of the parameters of the model within the models: Ununified SM, Li, Ma GN model, Topflavor model and No L-R 1 model.
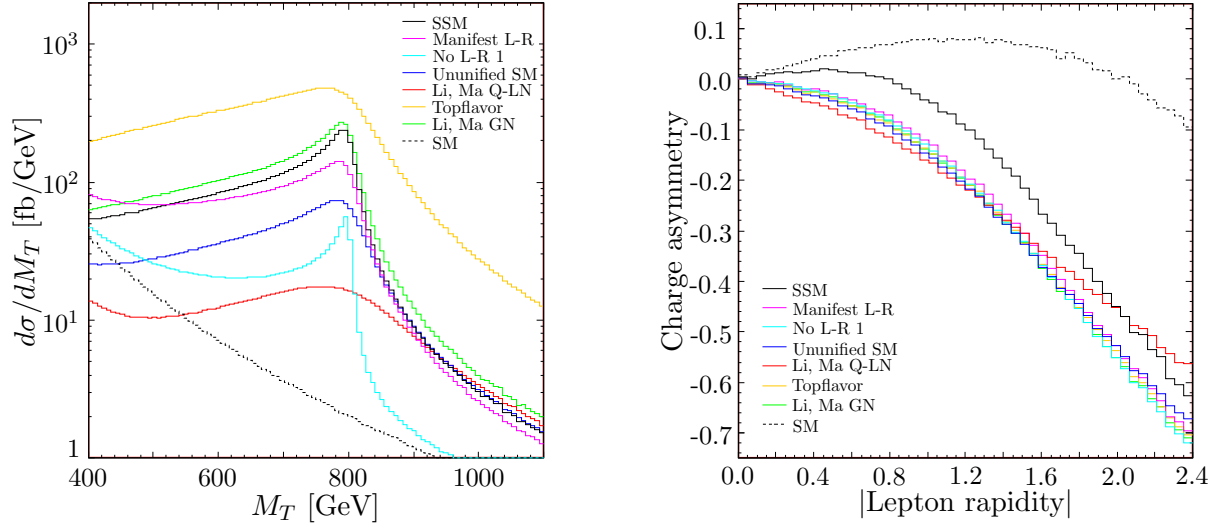
Figure 5.4: Transverse mass distribution and charge asymmetry as a function of the outgoing charged lepton rapidity at 10 TeV with $M_h = 800$GeV for different models under study. The "SM" label denotes the signal of the W^{SM} without the presence of a W' contribution.

Chapter 6

Summary and concluding remarks

As we mentioned in the introduction, it would be desirable to have a natural framework for describing possible deviation of the SM predictions with the experimental data. In this document we tried to create this framework for a general W′-boson predicted in the models based on an enlarged gauge group.

In Chapters 1 to 4 we have introduced a general W′-boson, reviewed models predicting it and derived a leading order formula for differential crosse section for its production and decay into the leptonic channel at LHC. In Chapter 5 we offered a description of an extension of the most cited leading order Monte Carlo generator `PYTHIA`, which was needed to account for the diversity of the W′-bosons predicted within the models mentioned in Chapter 3.

We believe, that we have succeeded in making the first step in a research of the implications of an additional charged vector bosons and that we have demonstrated the importance of this subject, particularly now as the LHC will be taken into operation in the fall of this year.

In the chapter on numerical results we have shown the effects of the interference, which was not accounted for in the original `PYTHIA` code at all and provided plots of the transverse mass distribution and the charge asymmetry in theories with an additional charged vectors boson based of an enlarged gauge group for chosen values of the parameters. In particular the mass of the heavy mass eigenstate of the system W^{SM} and W′ was set to a fixed value within all the models, to facilitate the comparison of predictions within different models.

In order to make this study complete, however, further work is needed. First of all the constraints on low-energy and electro-weak precision data need to be updated or derived in a model-independent manner. For that a classification of all the possible models predicting additional charged vector bosons needs to invented. A more systematic study of the implications of an additional W′-boson within the full parameter space of the different models is needed. Furthermore, to facilitate the distinction between different models the correlations of W′-boson with a Z'-boson should be investigated, since wherever a W′ is predicted there is also a Z'.

The predictions of other theories, not only SM model extensions based on an enlarged group, present a very interesting possibility for a future work on this subject as the energies at LHC will be probably high enough to probe new physics described by theories like Supersymmetry, Kaluza Klein, Technicolor and so on.

Bibliography

[1] T. Sjostrand, S. Mrenna, and P. Skands, "PYTHIA 6.4 Physics and Manual," *JHEP* **05** (2006) 026, `arXiv:hep-ph/0603175`.

[2] Particle Data Group Collaboration, C. Amsler *et al.*, "Review of particle physics," *Phys. Lett.* **B667** (2008) 1.

[3] K. S. Babu, X.-G. He, and E. Ma, "New Supersymmetric Left-Right Gauge Model: Higgs Boson Structure and Neutral Current Analysis," *Phys. Rev.* **D36** (1987) 878.

[4] A. Donini, F. Feruglio, J. Matias, and F. Zwirner, "Phenomenological aspects of a fermiophobic SU(2) x SU(2) x U(1) extension of the standard model," *Nucl. Phys.* **B507** (1997) 51–90, `arXiv:hep-ph/9705450`.

[5] P. Langacker and S. Uma Sankar, "Bounds on the Mass of W(R) and the W(L)-W(R) Mixing Angle xi in General SU(2)-L x SU(2)-R x U(1) Models," *Phys. Rev.* **D40** (1989) 1569–1585.

[6] G. Barenboim, J. Bernabeu, J. Prades, and M. Raidal, "Constraints on the W_R mass and CP violation in left- right models," *Phys. Rev.* **D55** (1997) 4213–4221, `arXiv:hep-ph/9611347`.

[7] H. Georgi, E. E. Jenkins, and E. H. Simmons, "The Ununified Standard Model," *Nucl. Phys.* **B331** (1990) 541.

[8] R. S. Chivukula, E. H. Simmons, and J. Terning, "Limits on the ununified standard model," *Phys. Lett.* **B346** (1995) 284–290, `arXiv:hep-ph/9412309`.

[9] X.-Y. Li and E. Ma, "Gauge model of quark lepton nonuniversality. ((U))," *Mod. Phys. Lett.* **A18** (2003) 1367–1376, `arXiv:hep-ph/0212029`.

[10] X.-y. Li and E. Ma, "Gauge model of generation nonuniversality reexamined," *J. Phys.* **G19** (1993) 1265–1278, `arXiv:hep-ph/9208210`.

[11] D. J. Muller and S. Nandi, "Top flavor: A Separate SU(2) for the third family," *Phys. Lett.* **B383** (1996) 345–350, `arXiv:hep-ph/9602390`.

[12] F. Halzen and A. D. Martin, "Quarks and Leptons: An introductory course in modern particle physics,". New York, Usa: Wiley (1984) 396p.

[13] R. K. Ellis, W. J. Stirling, and B. R. Webber, "QCD and collider physics," *Camb. Monogr. Part. Phys. Nucl. Phys. Cosmol.* **8** (1996) 1–435.

[14] T. G. Rizzo, "The Determination of the Helicity of W ' Boson Couplings at the LHC," *JHEP* **05** (2007) 037, `arXiv:0704.0235 [hep-ph]`.